Molecular architecture of copper(I) thiometallate complexes. Example of a cubane with an extra face, $(NPr_4)_3[MS_4Cu_4Cl_5]$ (M = Mo, W)

Yves Jeannin, Francis Sécheresse, Sylvain Bernès and Francis Robert
Laboratoire de Chimie des Métaux de Transition, Université Pierre et Marie Curie, 4 Place Jussieu, 75252 Paris Cédex 05 (France)

Abstract

Thiometallates MS_4^{2-} (M = Mo, W) form with copper(I) heterobimetallic complexes which are interesting because of the versatility of the structural types obtained. The various structures obtained by addition of copper(I) to MS_4^{2-} are described and illustrated by examples recently reported in the literature. The synthesis and structural characterization of $(NPr_4)_3[MS_4Cu_4Cl_5]$ are given together with the connections which exist between 'open' and 'closed' cubane structures.

Introduction

During the two last decades, owing to interest in bioinorganic chemistry and catalysis, research focused on producing Fe–S–Mo(W) compounds as synthetic models of the catalytic site of the enzyme nitrogenase, and on preparing transition metal complexes based on the $[Mo(W)S_4]^{2-}$ core, in connection with HDS catalytic activity. Indeed, this field has been reviewed extensively [1–11].

Motivations to study Cu–S–Mo(W) complexes, although quite different from those reported for Fe–Mo–S clusters, remain close to bioinorganic chemistry. After the first observations of Ferguson *et al.* [12] it appeared that the biological antagonism between copper and molybdenum was probably enhanced by the synergic effect of sulfur [13] as sulfate or thioamino acids. In fact, the so-called antagonism effect between $[MoS_4]^{2-}$ and Cu(I) on the metabolism of ruminants was clearly established [14].

Although Cu–Mo(W)–S clusters were less studied than Fe homologues, the versatility of the thiometallate ligands seems important enough in both cases to justify research on new structural modes. The various compounds recently characterized and built up on the potentially polydentate $[MS_4]^{2-}$ ligand and Cu(I) can be classified according to their Cu/M ratio. In Fig. 1 are represented the various structural types reported in the literature.

Cu/M = 1

Addition of a CuL group to $[MS_4]^{2-}$ (M = Mo, W) led to only one structural type with the copper atom bonded to the thiometallate across an S–S edge of the MS_4 tetrahedron (a). Complexes pertaining to this structural type were obtained by direct addition of CuL on $[MS_4]^{2-}$, $[CuCN(MoS_4)]^{2-}$ [15], $[CuSPh(MoS_4)]^{2-}$ and $[Cu(S\text{-}C_6H_4\text{-}p\text{-}Me)(MoS_4)]^{2-}$ [16]. With L = CN, the structural homologues with silver were also characterized, $[AgCN(MS_4)]^{2-}$, M = Mo [17, 18] and W [18].

Cu/M = 2

Formally two types of metallic frameworks are expected depending on the relative positions of the Cu atoms, which can be bonded to the MS_4 tetrahedron across two opposite edges, angle Cu–M–Cu = 180°, or across two adjacent edges, angle Cu–M–Cu = 90°. Generally the two Cu atoms adopt a trigonal planar geometry with a linear Cu–M–Cu skeleton as in type (b), $[Cu_2Cl_2(WS_4)]^{2-}$ [19], $[Cu_2Br_2(MoS_4)]^{2-}$ [20], $[Cu_2(SPh)_2(MoS_4)]^{2-}$ [16] and $[Cu_2(NCS)_2(WS_4)]^{2-}$ [21].

Substitution of the two terminal chloro ligands by phenanthroline did not modify the linear trimetallic enchainment showing the possibility for copper(I) to adopt trigonal or tetrahedral coordinations [22].

Similar distorted tetrahedral environments were also observed for Cu atoms bonded to monodentate ligands bridging two neighbouring units. $[Cu_2(CN)_2(MoS_4)]^{2-}$ [15] was isolated as zig-zag polymeric chains by formation of $Cu(\mu_2\text{-}CN)_2Cu$ bridges. In other examples, the two Cu atoms exhibit two types of geometries, trigonal planar and distorted tetrahedron (c). This geometry was obtained with M = Mo and L = PPh_3 [23] and for $[Ag_2(PPh_3)_3WSe_4]$ [24].

0020-1693/92/$5.00

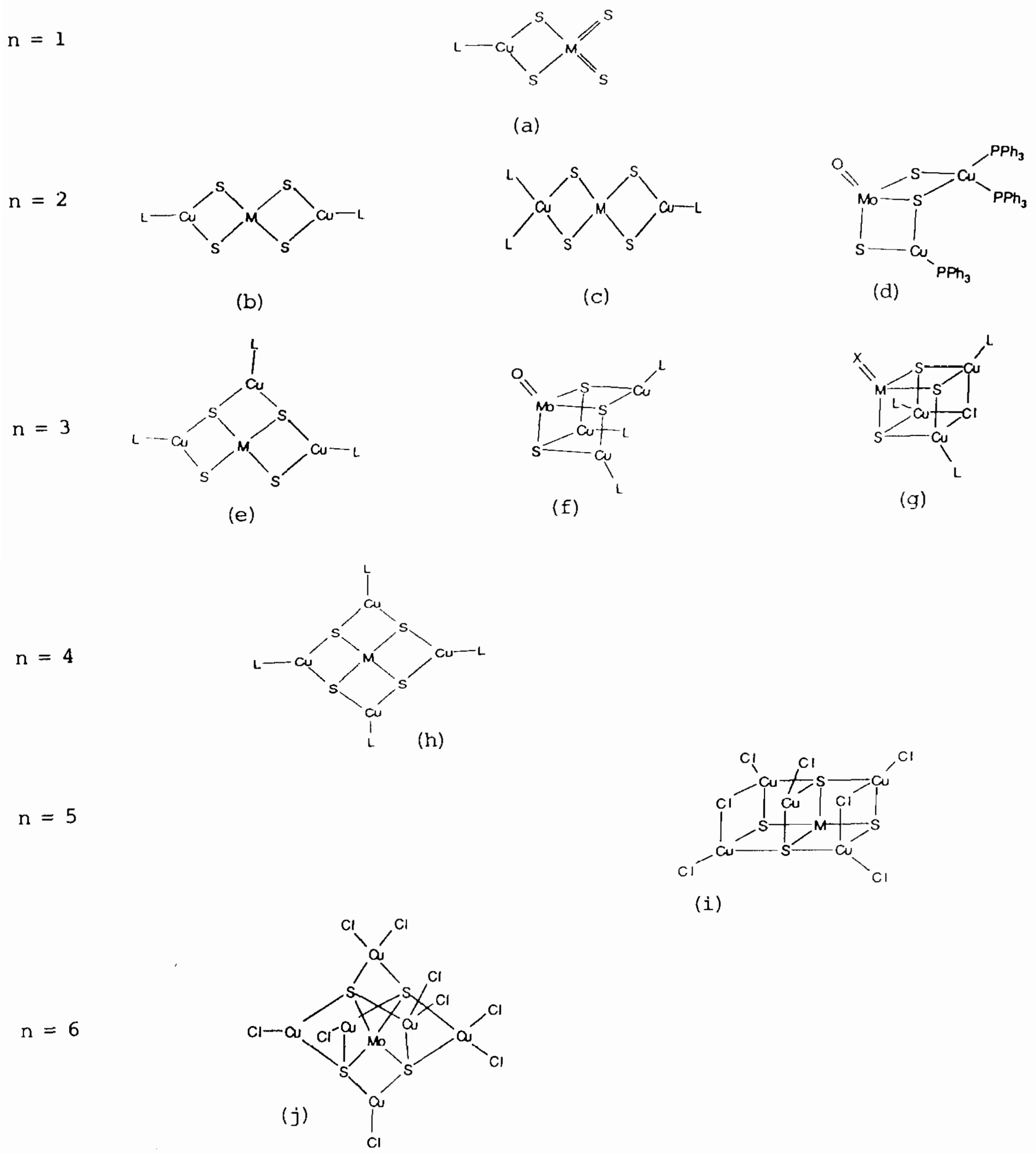

Fig. 1. Representation of the characterized structural types for complexes in which $[MS_4]^{2-}$ (M = Mo, W) served as a polydentate ligand. *n* represents the Cu/M ratio. Charges of the anions were omitted.

Only two examples of a 'bent' structure (d) are reported, both containing the oxotrithio fragment $[MoOS_3]^{2-}$. The stability of these complexes is probably related to the presence of a terminal oxygen which poorly bonds with weak acids such as Cu(I) [18].

The corresponding gold complex $[Au_2(PPh_3)_3MoS_3O]$ was also structurally characterized [25].

Cu/M = 3

A large set of compounds of this composition were prepared by direct addition of Cu(I) on $[MS_4]^{2-}$ or $[MS_3O]^{2-}$. Two different metallic enchainments are expected according to the relative positions of the Cu atoms bonded to the thiometallate.

The first structural mode (e) was obtained by addition of three Cu atoms on three S–S edges, angle Cu–M–Cu = 90°, the thiometallate ligand acting as a tetradentate ligand. Two sulfurs of the thiometallate are thrice bonded, the two others twice. This structural type was established for $[Cu_3Cl_3(MoS_4)]^{2-}$ [26], $[Cu_3Cl_3(WS_4)]^{2-}$ [27] and $[Cu_3Br_3(WS_4)]^{2-}$ [20]. Similarly to the case where Cu/M = 2, copper can adopt a distorted tetrahedral geometry without modification of the metallic core. This was obtained for $(NEt_4)_2$-$[Cu_3(NCS)_3WS_4]$ [28] where the NCS ambidentate ligands ensure bridges between two Cu atoms of two close units.

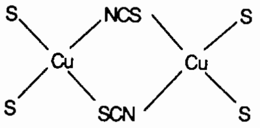

In the solid state, the structure of this compound was described as an inorganic infinite monodimensional polymer. Two of the three Cu atoms have tetragonal geometry resulting from $Cu(NCS)_2Cu$ bridges. Apart from being isolated by a polymerization process, Cu tetrahedral environments were also obtained with bidentate ligands such as dithiocarbamates (dtc), $[Cu_3(dtc\text{-}C_5H_{10})_3MS_4]^{2-}$ [29] and $[Cu_3(Et_2NCS_2)_3MoS_4]^{2-}$ [30].

The second structural mode encountered in complexes of ratio Cu/M = 3 results from the addition of three copper atoms on the thiometallate which therefore acts as a tridentate ligand. In the thiometallate, three sulfur atoms are involved in six equivalent Cu–S bonds, leaving the fourth free position available to participate in a terminal double bond. Compounds illustrating this chemical bonding observed in (f) were isolated only from $[MoS_3O]^{2-}$ which confirms the specific non-bonding behaviour of the terminal oxygen. Such a geometry was observed in $[Cu_3Cl_3MoS_3O]^{2-}$ [18] and $[Cu_3(NCS)_3MoS_3O]^{2-}$ [31]. In the latter, inter-aggregate Cu(NCS)Cu bridges led to a dimeric structure.

Addition of a supplementary ligand, bridging the three copper atoms of this structural type, produced the type (g) cubane structure $[Cu_3(PPh_3)_3ClMS_3X]$, X = O, S [32], which represents a structural analogue of cubanes isolated in the Fe–Mo–S series. This example illustrates the tendancy of copper(I) to form complexes with closed structure with thiometallates. This point was confirmed by the second compound $[Cu_4(PPh_3)_4S_6O_2W_2]$ [33], isolated in the synthesis of the former cubane, by reaction of $CuCl_2$ and PPh_3 on $Cs_2[WOS_3]$.

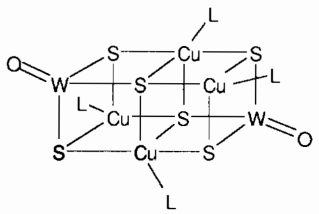

In the same way, analogues with $L = P(C_7H_7)_3$ [34] or copper replaced by silver [35] were characterized, $(Ph_2PMe)_4Ag_4W_2S_8$.

Cu/M = 4

Only the structural type (h) where thiometallates act as tetradentate ligands and give an 'open structure', is known. In the solid state $[Cu_4L_4MS_4]^{2-}$ was not isolated as a discrete species since the L ligands present in these complexes, L = Cl, Br [36, 37] and L = SCN [21, 28, 38], easily form $Cu(\mu_2\text{-}L)_2Cu$ bridges leading to the dimeric $[Cu_4Cl_4WS_4]_2{}^{4-}$ [36], linear polymeric $[Cu_4Br_4MoS_4]^{2-}$ [37], bidimensional $[Cu_4(SCN)_4MS_4]^{2-}$ [21, 28] and tridimensional $[Cu_4(SCN)_4WS_4]^{2-}$ [38]. Only one complex with unsymmetrically bonded copper atoms is reported, $[Cu_4(SCN)_5WS_4]^{3-}$ [28], polymerized through infinite linear chains, and showing large 12-membered rings. Recently the effect of the size of the countercations associated with the $[Cu_4Cl_4MS_4]^{2-}$ dianions on the dimensionality of the solids was illustrated [39].

Cu/M = 5

The only structurally characterized compounds are $[Cu_5Cl_7MS_4]^{4-}$, M = Mo [40], W [41], showing the double cubane-like structure (i) also observed in $[Cu_5Cl_7ReS_4]^{3-}$ [42].

Cu/M = 6

Recently the structure of $[Cu_6Cl_9MoS_4]^{5-}$ [43] was reported which represents the ultimate step of the addition of CuCl on thiometallates. The overall geometry (j) resulting from the saturation of the six S–S edges of the MS_4 tetrahedron by six CuCl groups is described as a distorted octahedron of coppers enclosing the tetrahedral thiometallate.

All types of structure described above were generally obtained by direct addition of CuCl on thiometallates. Another mode of synthesis was carried out by our group, based on addition (or excision) of CuCl on established structures. Because of the weak solubility of the molecular $[Cu_3(PPh_3)_3ClMS_4]$ [32] cubanes, our first purpose was to prepare soluble cubanes by replacing the terminal neutral PPh_3 groups by anionic ligands. Then controlled addition of CuCl and chlorides on those soluble species allowed isolation of both open and closed new structural types. Those syntheses by 'block-assembly' were applied to the cubane structure (g) which shows the possibility, through the free terminal W=S bond, of adding a supplementary CuCl group to yield a new closed structure of higher nuclearity. Regarding the cubane structure (g), three isomers are expected according to the S–S edge of addition as represented in the following diagram. Conversely, from the open model (h) $[Cu_4Cl_4MS_4]^{2-}$ soluble closed cubane geometry (g) of lower nuclearity was also isolated.

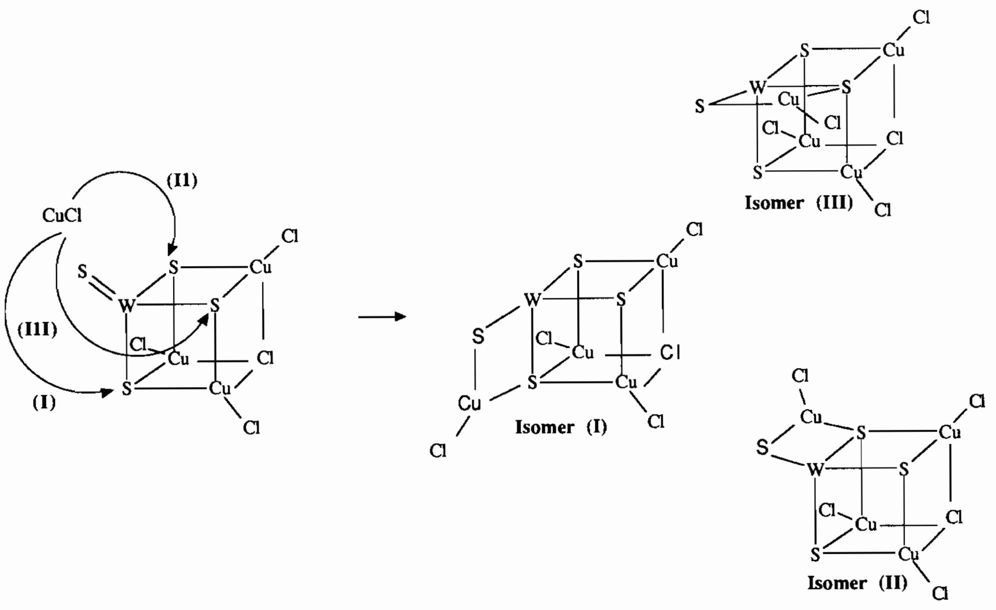

Experimental

Preparations of compounds

*$(NEt_4)_3[WS_4Cu_3Cl_4]NEt_4Cl$ (**1a**)*

Copper(I) chloride (0.075 g, 0.75 mmol) and tetraethylammonium chloride (0.125 g, 0.75 mmol) were added to a solution of 50 ml of $(NEt_4)_2[WS_4]$ (0.143 g, 0.25 mmol) in dichloromethane. The resulting orange solution was refluxed for 20 min, cooled to room temperature, and then concentrated to *c.* 10 ml under reduced pressure. Ether was added to the solution and storage at room temperature for 24 h afforded 0.030 g of orange crystals. *Anal.* Calc. for $C_{32}H_{80}Cl_5Cu_3N_4S_4W$ (**1a**): C, 32.00; H, 6.70; Cl, 14.80; N, 4.70; S, 10.67. Found: C, 32.08; H, 6.69; Cl, 17.4; N, 4.78; S, 10.00%.

*$(NEt_4)_3[MoS_4Cu_3Cl_4]NEt_4Cl$ (**1b**)*

To a solution of $(NBu_4)_2[MoS_4Cu_4Cl_4]$ [39] (0.221 g, 0.2 mmol) in 40 ml of dichloromethane was added NEt_4Cl (0.200 g, 1.2 mmol). After 30 min of stirring the violet solution was filtered, concentrated under reduced pressure to *c.* 20 ml and ether was added prior to standing several days at room temperature. Violet crystals were collected, washed with ether and analyzed. *Anal.* Calc. for $C_{32}H_{80}Cl_5Cu_3MoN_4S_4$ (**1b**): C, 34.53; H, 7.19; Cl, 15.96; Cu, 17.13; Mo, 8.63; N, 5.03; S, 11.51. Found: C, 32.33; H, 7.10; Cl, 16.23; Cu, 15.80; Mo, 8.60; N, 4.82; S, 9.20%.

*$(NPr_4)_3[WS_4Cu_3Cl_4]$ (**2a**)*

To a stirred solution of $(NPr_4)_2[WS_4]$ (0.170 g, 0.25 mmol) in 70 ml of dichloromethane was added CuCl (0.075 g, 0.75 mmol). After addition of freshly prepared NPr_4Cl (0.177 g, 0.80 mmol) the resulting orange solution was refluxed for 45 min. After cooling to room temperature the solid formed was eliminated by filtration and ether added to the filtrate prior to standing at room temperature for several days. Yield 0.100 g of red crystals. *Anal.* Calc. for $C_{36}H_{84}Cl_4Cu_3N_3S_4W$ (**2a**): C, 35.92; H, 6.98; Cl, 11.81; Cu, 15.85; N, 3.49; S, 10.64; W, 15.30. Found: C, 35.94; H, 6.95; Cl, 11.92; Cu, 15.30; N, 3.52; S, 10.40; W, 14.53%.

*$(NPr_4)_3[MoS_4Cu_3Cl_4]$ (**2b**)*

Compound **2b** was obtained by a similar route to **2a** starting from $(NPr_4)_2[MoS_4]$ (0.150 g, 0.25 mmol). Yield 0.130 g of violet crystals. *Anal.* Calc. for $C_{36}H_{84}Cl_4Cu_3MoN_3S_4$: C, 38.76; H, 7.54; Cl, 12.74; Cu, 17.09; Mo, 8.61; N, 3.77; S, 11.48. Found: C, 37.46; H, 7.46; Cl, 12.82; Cu, 17.86; Mo, 8.54; N, 3.58; S, 11.25%.

*$(NPr_4)_2[MOS_3Cu_3Cl_3]$ ($M = W$ (**3a**), Mo (**3b**))*

After elimination of **2a** and **2b** yellow crystals of **3a** or violet crystals of **3b** deposited in the filtrates. They were identified by X-ray measurements.

*$[MS_4Cu_3(PPh_3)_3Cl]$ ($M = W$ (**4a**), Mo (**4b**))*

To a solution of **2a** (0.120 g, 0.10 mmol) in 30 ml of acetonitrile was added PPh_3 (0.210 g, 0.8 mmol). After 30 min of stirring at room temperature the solution was filtered and concentrated by slow evaporation until yellow crystals deposited. The same route was used to prepare **4b**. The two reaction products **4a** and **4b** were characterized by their crystallographic cell dimensions and spectral features.

$(NPr_4)_3[WS_4Cu_4Cl_5]$ (5a)

To a solution of $(NPr_4)_3[WS_4Cu_3Cl_4]$ (**2a**) (0.085 g, 0.070 mmol) in 20 ml of dichloromethane was added a suspension of CuCl (0.007 g, 0.07 mmol) in dichloromethane. After 30 min of stirring at room temperature, the mixture was filtered and the filtrate reduced to *c*. 10 ml. Addition of ether to the filtrate and standing for 24 h at room temperature afforded two types of red crystals characterized by single-crystal X-ray analysis. Small red crystals were identified as $(NPr_4)_2[WS_4Cu_4Cl_4]$ [39] and large red platelets as $(NPr_4)_3[WS_4Cu_4Cl_5]$ (**5a**). Owing to the mixture of crystals obtained via this route, a direct and selective preparation was also carried out.

A mixture of $(NPr_4)_2[WS_4]$ (0.340 g, 0.5 mmol) and CuCl (0.150 g, 1.50 mmol) in 50 ml of dichloromethane was stirred at room temperature for 20 min. The orange–red suspension thus obtained was filtered and then the solvent evaporated under reduced pressure. The crude product was recrystallized from dichloromethane. Within a few days at room temperature 0.250 g of red crystals were collected. *Anal.* Calc. for $C_{36}H_{84}Cl_5Cu_4N_3S_4W$ (**5a**): C, 33.19; H, 6.45; Cl, 13.64; Cu, 19.51; N, 3.23; S, 9.83; W, 14.14. Found: C, 32.98; H, 6.57; Cl, 13.52; Cu, 19.40; N, 3.01; S, 9.73; W, 14.15%.

$(NPr_4)_3[MoS_4Cu_4Cl_5]$ (5b)

Pure compound **5b** was obtained in a similar manner to **5a** starting from $(NPr_4)_2[MoS_4]$ (0.300 g, 0.5 mmol) and CuCl (0.150 g, 1.5 mmol) yielding 0.130 g of violet crystals. *Anal.* Calc. for $C_{36}H_{84}Cl_5Cu_4MoN_3S_4$ (**5b**): C, 35.60; H, 6.92; Cl, 14.63; Cu, 20.93; Mo. 7.92; N, 3.46; S, 10.55. Found: C, 35.60; H, 6.80; Cl, 14.64; Cu, 21.17; Mo, 8.13; N, 4.09; S, 10.56%.

Crystal structure determination

Unit cell parameters for all compounds were obtained from least-squares refinement of the positions of 25 reflections. Intensity data were collected at room temperature with a θ–2θ scan technique. Corrections for polarization and Lorentz effects were applied. For all compounds an absorption correction based on the DIFABS program [44] was performed. The structures of **1a**, and **3a** were solved by direct methods [45], **5a** by Patterson maps. After location of metallic centres, all remaining non-hydrogen atoms were located with use of successive difference Fourier maps. All atom parameters were refined using CRYSTALS program [46]; hydrogen contributions were omitted. Calculations were performed with a Micro Vax II computer. Crystal parameters, details of the data collection, and final *R* factors are given in Table 1.

$(NEt_4)_3[WS_4Cu_3Cl_4]NEt_4Cl$ (1a)

The systematic absences *hhl* ($l=2n+1$), and *h*00 ($h=2n+1$) together with evidence of a non-centrosymmetric group define the space group $P\bar{4}2_1c$. The structural determination led to a 12-site mean structure generated through the $\bar{4}$ axis by the three basic peaks, namely 1,2,3 as represented in the following drawing.

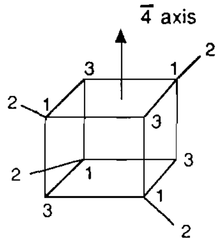

Sites 3 exhibit electronic densities consistent with the presence of a sulfur or a chlorine atom. Each of sites 1 and 2 contains two atoms in statistical disorder, W and Cu for 1, Cl and S for 2. Refinement of the occupancy factors of each site converged to the statistical values of three coppers and a tungsten for sites 1, and three chlorines and a sulfur for sites 2. Moreover, positions of atoms in each site were clearly separated giving a W–Cu separation of 0.390(7) Å and a S–Cl separation of 0.38(4) Å.

Owing to the chemical analysis, the atom located in site 2 and bonded to the tungsten atom of site 1 was obviously identified as a sulfur atom and in the same way, the atom of site 3, bonded to three copper atoms of site 1 was identified as a chlorine atom. Comparison of these results with the bond angle values given in Table 5 led to the cubic geometry represented below.

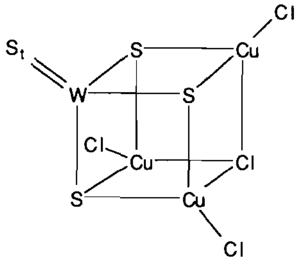

The statistical distribution observed in the fragment of the structure can be represented by a stacking defect. The basic cubic anion can rotate around each of the three $\bar{4}$ axes of the cube passing through the centre of the faces, the superposition of these various configurations yielding the statistical crystallographic model.

The structure of **1a** is achieved by an additional NEt_4Cl molecule with the Cl atom located on the $\bar{4}$ axis and the $NEt_4{}^+$ cation in a general position. All atoms of the structure were refined anisotropically. After the final cycle a residue of 0.45 e/Å^3 was observed at 1.57 Å from the W atom. The final positional parameters with e.s.d.s are given in Table 2.

TABLE 1. Crystallographic data, intensity measurements and refinement parameters for $(NEt_4)_3[WS_4Cu_3Cl_4]NEt_4Cl$ (**1a**), $(NPr_4)_2[MS_3OCu_3Cl_3]$ (**3a**, **3b**) and $(NPr_4)_3[MS_4Cu_4Cl_5]$ (**5a**, **5b**), M=Mo, W

	1a	**3a**	**3b**	**5a**	**5b**
Crystallographic data					
Formula	$C_{32}H_{80}N_4Cl_5S_4Cu_3W$	$C_{24}H_{56}N_2Cl_3S_3OCu_3W$	$C_{24}H_{56}N_2Cl_3S_3OCu_3Mo$	$C_{36}H_{84}N_3Cl_5S_4Cu_4W$	$C_{36}H_{84}N_3Cl_5S_4Cu_4Mo$
Molecular weight	1201	965.7	877.8	1302.6	1212.7
Crystal system	tetragonal	monoclinic	monoclinic	monoclinic	monoclinic
Space group	$P\bar{4}2_1c$	$P2_1/a$	$P2_1/a$	$P2_1$	$P2_1$
a (Å)	12.329(1)	16.941(3)	16.932(3)	11.4519(7)	11.419(4)
b (Å)		12.691(2)	12.676(3)	20.940(2)	20.877(8)
c (Å)	16.255(3)	17.634(3)	17.626(3)	11.665(1)	11.631(4)
α (°)	90	90	90	90	90
β (°)	90	93.55(2)	93.60(1)	90.05(6)	90.06(3)
γ (°)	90	90	90	90	90
V (Å^3)	2471(1)	3784(4)	3776(3)	2797.4(4)	2773(2)
Z	2	4	4	2	2
ρ_{calc} (g cm^{-3})	1.61	1.69	1.54	1.55	1.45
$F(000)$	1220	1928	1800	1320	1256
Data collection and refinement parameters					
Diffractometer	Enraf-Nonius CAD4	Enraf-Nonius CAD4	Enraf-Nonius CAD4	Enraf-Nonius CAD4	Enraf-Nonius CAD4
Radiation	Mo Kα (λ=0.71069 Å)	Mo Kα (λ=0.71069 Å)	Mo Kα (λ=0.71069 Å)	Mo Kα (λ=0.71069 Å)	Mo Kα (λ=0.71069 Å)
μ (Mo, Kα) (cm^{-1})	41.1	51.6		40.06	
Scan mode	$\theta/2\theta$	$\theta/2\theta$		$\theta/2\theta$	
Scan width	0.90+0.345 tan θ	0.90+0.345 tan θ		0.90+0.345 tan θ	
θ-Range	1–25	1–25		1–25	
Octants recorded	$+h$, $+k$, $+l$	$\pm h$, $+k$, $+l$		$\pm h$, $+k$, $+l$	
Data collected	2489	5906		5334	
Unique data	1239	5346		5076	
Data used in refinement $(F_o)^2>3\sigma(F_o^2)$	821	3281		4698	
R (%)	5.23	5.12		7.31	
R_w (%)	5.08	6.26		7.34	
Absorption correction	Difabs	Difabs		Difabs	
Transmission factors	0.794–1.146	0.995–1.191		0.785–1.346	
No. variables	138 (4 blocks)	234 (4 blocks)		480 (5 blocks)	
Weighting scheme	Chebyshev	Chebyshev		Chebyshev	
Coefficients	8.28; −5.28; 6.72	5.65; −0.26; 3.47		10.40; −4.36; 7.34	
Secondary ext. (10^{-6})	26.3	136.0		122.4	

TABLE 2. Fractional atomic coordinates with their e.s.d.s for $(NEt_4)_3[WS_4Cu_3Cl_4]NEt_4Cl$ (**1a**)

Atom	x/a	y/b	z/c	U_{eq}	Occupancy
W(1)	0.0290(3)	−0.0956(4)	0.0543(2)	0.0275	0.25
S(1)	−0.1415(2)	−0.0442(2)	0.0788(2)	0.0384	
Cu(1)	0.0420(5)	−0.1184(4)	0.0677(4)	0.0644	0.75
Cl(1)	0.0815(9)	−0.2516(6)	0.1492(8)	0.0532	0.75
S(2)	0.069(3)	−0.240(3)	0.130(2)	0.0779	0.25
Cl(2)	0.00000	−0.00000	0.50000	0.0430	
N(1)	0.2592(7)	−0.0832(7)	0.3482(5)	0.0390	
C(1)	0.1612(9)	−0.031(1)	0.3123(8)	0.0428	
C(2)	0.161(1)	0.0917(9)	0.3083(9)	0.0574	
C(3)	0.3603(9)	−0.056(1)	0.2994(8)	0.0483	
C(4)	0.358(1)	−0.088(1)	0.2097(8)	0.0598	
C(5)	0.274(1)	−0.042(1)	0.438(1)	0.0606	
C(6)	0.358(1)	−0.106(2)	0.4884(8)	0.0691	
C(7)	0.242(1)	−0.2072(9)	0.3447(9)	0.0486	
C(8)	0.149(1)	−0.243(1)	0.399(1)	0.0742	

$(NPr_4)_3[WS_4Cu_3Cl_4]$ (2a)

The structure of **2a** was not refined because of a statistical disorder of the same type as in compound **1a**. Nevertheless the cubane structure was assumed according to the crystallographic data (cubic system, $a = 11.560(5)$ Å), spectroscopic data and chemical reactivity.

$(NPr_4)_2[WOS_3Cu_3Cl_3]$ (3a)

Since compounds **3a** and **3b** are isomorphous only the structure of **3a** was solved. The systematic absences $h0l$ ($h = 2n+1$) and $0k0$ ($k = 2n+1$) uniquely define the space group $P2_1/a$. One of the two cations is disordered. The C(21), C(22), C(24), C(25), C(27), C(28) and C(30) atoms are located in their sites with an occupancy of 0.66, the corresponding disordered positions C(211) to C(301) with an occupancy of 0.34. In the refinement, anisotropic temperature factors were attributed to all atoms of the anion, W, O, S, Cu, Cl, whereas isotropic temperature factors were used for the cations. A final difference Fourier map revealed a peak (1.7 e/Å^3) near the W atom. The final positional parameters with their e.s.d.s. are listed in Table 3.

$(NPr_4)_3[WS_4Cu_4Cl_5]$ (5a)

Since compounds **5a** and **5b** are isomorphous, only the structure of **5a** was solved. Angles between the cell axes are close to 90°, but the binary axis of a monoclinic system was unambiguously evidenced from Laue equivalent intensities. The $P2_1$ space group was chosen in agreement with the systematic absences $0k0$ ($k = 2n+1$), and lack of centrosymmetry. Anisotropic temperature factors were used for all atoms. A final difference Fourier map showed a peak of 3.2 e/Å^3 located at 2.72 Å from the W atom which was not attributed. Fractional atomic parameters are listed in Table 4.

TABLE 3. Fractional atomic coordinates with their e.s.d.s for $(NPr_4)_2[WOS_3Cu_3Cl_3]$ (**3a**)

Atom[a]	x/a	y/b	z/c	U_{eq}	U_{iso}
W(1)	0.49886(3)	0.12862(3)	0.75886(3)	0.0437	
S(1)	0.5119(2)	0.3062(2)	0.7738(2)	0.0526	
S(2)	0.5756(2)	0.0510(2)	0.8522(2)	0.0526	
S(3)	0.5454(2)	0.0828(2)	0.6458(2)	0.0520	
O(1)	0.4035(6)	0.0902(7)	0.7627(6)	0.0687	
Cu(1)	0.58647(9)	0.2264(1)	0.8670(1)	0.0511	
Cu(2)	0.56037(9)	0.2594(1)	0.6615(1)	0.0511	
Cu(3)	0.61555(9)	−0.0054(1)	0.7393(1)	0.0532	
Cl(1)	0.6473(2)	0.3047(3)	0.9615(2)	0.0663	
Cl(2)	0.6066(2)	0.3637(3)	0.5789(3)	0.0689	
Cl(3)	0.6998(2)	−0.1290(3)	0.7264(3)	0.0702	
N(1)	0.3982(5)	0.3104(7)	1.0668(6)		0.046(2)
C(1)	0.3646(7)	0.2032(9)	1.0398(8)		0.051(3)
C(2)	0.4101(9)	0.156(1)	0.973(1)		0.068(4)
C(3)	0.3649(9)	0.051(1)	0.949(1)		0.072(4)
C(4)	0.3970(7)	0.3932(9)	1.0015(8)		0.052(3)
C(5)	0.3163(8)	0.409(1)	0.9589(9)		0.066(4)
C(6)	0.3276(9)	0.485(1)	0.893(1)		0.083(5)
C(7)	0.4846(7)	0.3018(9)	1.0936(8)		0.052(3)
C(8)	0.5010(9)	0.225(1)	1.163(1)		0.071(4)
C(9)	0.591(1)	0.216(1)	1.177(1)		0.083(5)
C(10)	0.3435(8)	0.342(1)	1.1292(9)		0.058(3)
C(11)	0.3687(9)	0.444(1)	1.172(1)		0.079(5)
C(12)	0.310(1)	0.460(1)	1.235(1)		0.093(5)
N(2)	0.3160(6)	0.3717(8)	0.5600(6)		0.049(2)
C(21)*	0.348(2)	0.265(3)	0.521(2)		0.103(9)
C(22)*	0.390(2)	0.277(3)	0.457(2)		0.12(1)
C(23)	0.438(1)	0.179(1)	0.442(1)		0.093(5)
C(24)*	0.382(2)	0.445(2)	0.580(2)		0.092(8)
C(25)*	0.367(2)	0.535(3)	0.625(2)		0.12(1)
C(26)	0.430(1)	0.611(2)	0.649(1)		0.129(8)
C(27)*	0.261(1)	0.425(2)	0.496(2)		0.077(7)
C(28)*	0.202(2)	0.368(3)	0.452(2)		0.104(9)
C(29)	0.147(1)	0.428(2)	0.402(1)		0.107(6)
C(30)*	0.315(2)	0.299(2)	0.646(2)		0.078(7)
C(31)	0.269(2)	0.339(2)	0.692(2)		0.149(9)
C(32)	0.2564(9)	0.266(1)	0.756(1)		0.073(4)
C(211)**	0.383(2)	0.337(2)	0.516(2)		0.035(7)
C(221)**	0.370(2)	0.213(3)	0.489(3)		0.06(1)
C(241)**	0.331(1)	0.490(2)	0.583(2)		0.023(5)
C(251)**	0.414(2)	0.506(3)	0.635(2)		0.039(8)
C(271)**	0.235(2)	0.369(2)	0.522(2)		0.026(6)
C(281)**	0.232(2)	0.429(3)	0.437(3)		0.05(1)
C(301)**	0.259(2)	0.342(2)	0.615(2)		0.031(7)

[a]Single asterisk: occupancy 0.66; double asterisk: occupancy 0.34.

Results and discussion

Crystal structures

$[WS_4Cu_3Cl_4]^{3-}$ (1a)

An ORTEP drawing of **1a** is given in Fig. 2 including the labelling scheme. Selected bond distances and angles

TABLE 4. Fractional atomic coordinates with their e.s.d.s for $(NPr_4)_3[WS_4Cu_4Cl_5]$ (**5a**)

Atom	*x/a*	*y/b*	*z/c*	U_{eq}
W(1)	0.15011(4)	0.00093(7)	0.25343(4)	0.0353
S(1)	−0.0051(4)	−0.0080(3)	0.3672(4)	0.0563
S(2)	0.0970(4)	−0.0004(3)	0.0707(3)	0.0555
S(3)	0.2708(4)	−0.0811(2)	0.2887(4)	0.0441
S(4)	0.2432(5)	0.0930(2)	0.2906(4)	0.0476
Cu(1)	0.2537(3)	−0.0699(1)	0.0900(2)	0.0651
Cu(2)	0.3814(2)	0.0133(1)	0.2885(2)	0.0571
Cu(3)	0.2153(3)	0.0850(1)	0.0975(2)	0.0615
Cu(4)	0.1047(2)	−0.0963(1)	0.3908(2)	0.0525
Cl(1)	0.2885(6)	−0.1492(3)	−0.0268(5)	0.0718
Cl(2)	0.5336(4)	0.0202(3)	0.4047(5)	0.0687
Cl(3)	0.2205(7)	0.1610(3)	−0.0272(5)	0.0745
Cl(4)	0.0689(5)	−0.1796(3)	0.4913(5)	0.0729
Cl(5)	0.4319(4)	0.0075(4)	0.0836(4)	0.0720
N(1)	0.741(1)	0.5126(9)	0.306(1)	0.0507
C(1)	0.838(2)	0.4830(8)	0.227(1)	0.0547
C(2)	0.941(2)	0.454(2)	0.296(2)	0.0753
C(3)	1.030(2)	0.434(1)	0.206(2)	0.0817
C(4)	0.650(2)	0.536(1)	0.224(2)	0.0601
C(5)	0.541(2)	0.568(2)	0.283(2)	0.0757
C(6)	0.457(3)	0.582(2)	0.186(2)	0.1005
C(7)	0.783(2)	0.561(1)	0.389(2)	0.0638
C(8)	0.845(3)	0.616(1)	0.331(2)	0.0776
C(9)	0.891(4)	0.661(2)	0.425(3)	0.1067
C(10)	0.690(2)	0.4586(9)	0.389(2)	0.0603
C(11)	0.628(2)	0.402(1)	0.324(2)	0.0734
C(12)	0.592(2)	0.355(1)	0.419(3)	0.0854
N(3)	0.784(1)	0.1722(6)	0.224(1)	0.0431
C(31)	0.785(1)	0.1311(9)	0.337(2)	0.0537
C(32)	0.757(2)	0.164(1)	0.439(2)	0.0640
C(33)	0.775(2)	0.125(1)	0.539(3)	0.0845
C(34)	0.670(2)	0.2106(9)	0.205(2)	0.0546
C(35)	0.558(3)	0.170(1)	0.201(4)	0.0929
C(36)	0.457(2)	0.216(1)	0.191(3)	0.0916
C(37)	0.810(2)	0.126(1)	0.129(2)	0.0670
C(38)	0.812(3)	0.158(1)	0.010(2)	0.0933
C(39)	0.861(4)	0.113(2)	−0.077(2)	0.1082
C(40)	0.880(1)	0.2245(9)	0.235(2)	0.0520
C(41)	1.003(2)	0.200(1)	0.243(2)	0.0660
C(42)	1.091(2)	0.251(1)	0.249(3)	0.0821
N(5)	0.293(1)	0.3366(7)	0.783(1)	0.0494
C(51)	0.279(2)	0.3801(9)	0.676(1)	0.0551
C(52)	0.275(3)	0.341(1)	0.565(3)	0.0903
C(53)	0.247(2)	0.397(1)	0.465(2)	0.0731
C(54)	0.386(2)	0.287(1)	0.766(2)	0.0610
C(55)	0.511(2)	0.316(1)	0.752(3)	0.0743
C(56)	0.597(3)	0.266(2)	0.731(4)	0.1090
C(57)	0.182(2)	0.302(1)	0.808(2)	0.0607
C(58)	0.074(2)	0.336(1)	0.834(3)	0.0848
C(59)	−0.027(2)	0.290(1)	0.835(4)	0.0917
C(60)	0.316(3)	0.383(1)	0.883(2)	0.0754
C(61)	0.331(3)	0.349(1)	0.997(3)	0.0927
C(62)	0.363(3)	0.399(1)	1.096(2)	0.0935

are given in Table 5. The W atom has retained the tetrahedral geometry of the free $[WS_4]^{2-}$ ligand with S–W–S angles ranging from 108.2(2) to 112.3(8)°. Three CuCl groups are bonded to the WS_4 tetrahedron across

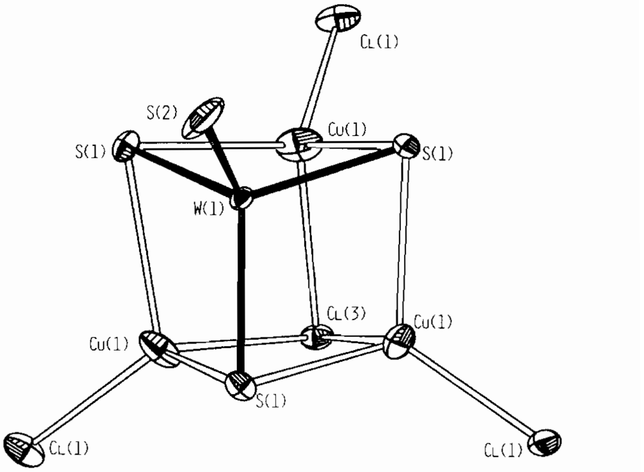

Fig. 2. ORTEP drawing (15% ellipsoids) of the $[WS_4Cu_3Cl_4]^{3-}$ cubane anion. Disordered positions were omitted for clarity.

TABLE 5. Selected bond distances (Å) and angles (°) for the $[WS_4Cu_3Cl_4]^{3-}$ anion in **1a**

W(1)–S(1)	2.232(5)	W(1)···Cu(1)	2.833(6)
W(1)–S(1)	2.248(5)	W(1)···Cu(1)	2.770(7)
W(1)–S(1)	2.244(5)	W(1)···Cu(1)	2.788(4)
W(1)–S(2)	2.22(4)	Cu(1)–Cl(1)	2.17(1)
S(1)–Cu(1)	2.447(7)		
S(1)–Cu(1)	2.399(7)		
S(1)–Cu(1)	2.357(7)		
S(1)–W(1)–S(1)	109.4(2)	S(2)–W(1)–S(1)	109.8(10)
S(1)–W(1)–S(1)	108.8(2)	S(2)–W(1)–S(1)	112.3(8)
S(1)–W(1)–S(1)	108.2(2)	S(2)–W(1)–S(1)	108.4(11)
Cu(1)–S(1)–W(1)	74.2(2)	Cu(1)–S(1)–W(1)	72.7(2)
Cu(1)–S(1)–W(1)	73.4(2)	Cu(1)–S(1)–W(1)	75.1(2)
Cu(1)–S(1)–W(1)	74.8(2)	Cu(1)–S(1)–W(1)	74.0(2)
Cl(1)–Cu(1)–S(1)	116.5(5)	Cl(1)–Cu(1)–S(1)	118.7(3)
Cl(1)–Cu(1)–S(1)	121.0(4)	S(1)–Cu(1)–S(1)	97.4(2)
S(1)–Cu(1)–S(1)	99.1(2)		
S(1)–Cu(1)–S(1)	99.9(3)		

three edges, two of which have a common vertex. The Cu(1)–Cl(1) distances of 2.17(1) Å are those expected for terminal chloro–copper bonds [28].

The mode of coordination of copper chloride led to the distinction of two types of S atoms in **1a**.

(i) A terminal S_t atom, bonded to only the W atom but showing a long $W{=}S_t$ distance of 2.22(4) Å with respect to the 2.14 Å usually reported for such types of double bond [32]. Nevertheless the value of this lengthening remains lower than 2σ. The high value of the error on this distance is probably a consequence of the disorder on the S_t and Cl positions.

(ii) Three bridging S atoms are bonded to the tungsten and to two copper atoms. W–S distances ranging from 2.232(5) to 2.248(5) Å are in good agreement with the values reported for this type of bond [32]. Conversely Cu–S bonds, 2.357(7)–2.447(7) Å, are longer than usually observed in similar enchainments. This lengthening is probably the origin of the observed increase of the distances between the metallic centres in the Cu_3WS_4 fragment. The geometry of the anion is completed by a fourth chlorine bridging three Cu atoms.

The geometry of the three equivalent copper atoms is distorted from the ideal tetrahedron with angles at the Cu atoms in the range 97.4(2)–121.0(4)°. The 12-atom cage $[WS_4Cu_3Cl_4]^{3-}$ can be represented by a distorted cube bearing four terminal atoms, three chlorines and a sulfur atom.

$(NPr_4)_2[WOS_3Cu_3Cl_3]$ (3a)

Selected bond distances and angles of the anion are listed in Table 6. Anion **3a** represents the homologue with tungsten of the Mo compound $(PPh_4)_2$-$[MoOS_3Cu_3Cl_3]$ isolated by Müller *et al.* [18]. An oxygen and three sulfur atoms are bonded to the central tungsten.

The W=O distance of 1.69(1) Å is characteristic of a pure double bond, and consistent with the values reported for related cubic structures (g), such as $[WOS_3Cu_3(PPh_3)_3Cl]$ [32]. The three long W–S distances, 2.259(3)–2.278(3) Å, confirm that the three S atoms are engaged in single bonds. The three Cu atoms are linked to the WS_3 core across symmetrical double bridges with all Cu–S distances in the short range 2.247(3)–2.270(3) Å. The geometry of the Cu_3WS_3 fragment can be described as an incomplete cube with three terminal Cu–Cl bonds as shown in Fig. 3. Though the Cu atoms are crystallographically independent, they exhibit the same trigonal planar environment.

TABLE 6. Selected bond distances (Å) and angles (°) for the $[WOS_3Cu_3Cl_3]^{2-}$ anion in **3a**

W(1)–S(1)	2.278(3)	W(1)–S(2)	2.259(3)
W(1)–S(3)	2.264(4)	W(1)–O(1)	1.69(1)
W(1)...Cu(1)	2.651(2)		
W(1)...Cu(2)	2.647(2)		
W(1)...Cu(3)	2.647(2)		
S(2)–W(1)–S(1)	107.4(1)	O(1)–W(1)–S(1)	111.5(3)
S(3)–W(1)–S(1)	108.6(1)	O(1)–W(1)–S(2)	110.7(4)
S(3)–W(1)–S(2)	108.3(1)	O(1)–W(1)–S(3)	110.2(4)
Cu(2)–W(1)–Cu(1)	87.00(5)		
Cu(3)–W(1)–Cu(1)	90.29(5)		
Cu(3)–W(1)–Cu(2)	89.49(5)		
S(1)–Cu(1)	2.250(4)	S(1)–Cu(2)	2.268(4)
S(2)–Cu(1)	2.247(3)	S(2)–Cu(3)	2.260(4)
S(3)–Cu(2)	2.270(3)	S(3)–Cu(3)	2.267(4)
Cu(1)–S(1)–W(1)	71.7(1)	Cu(1)–S(2)–W(1)	72.1(1)
Cu(2)–S(1)–W(1)	71.2(1)	Cu(3)–S(2)–W(1)	71.7(1)
Cu(2)–S(1)–Cu(1)	107.6(1)	Cu(3)–S(2)–Cu(1)	112.9(2)
Cu(2)–S(3)–W(1)	71.4(1)		
Cu(3)–S(3)–W(1)	71.5(1)		
Cu(3)–S(3)–Cu(2)	110.4(1)		
Cu(1)–Cl(1)	2.149(4)	Cu(2)–Cl(2)	2.152(4)
Cu(3)–Cl(3)	2.142(4)		
S(2)–Cu(1)–S(1)	108.8(1)	S(3)–Cu(2)–S(1)	108.7(1)
Cl(1)–Cu(1)–S(1)	125.4(1)	Cl(2)–Cu(2)–S(1)	126.6(2)
Cl(1)–Cu(1)–S(2)	125.5(2)	Cl(2)–Cu(2)–S(3)	124.5(2)
S(3)–Cu(3)–S(2)	108.2(1)		
Cl(3)–Cu(3)–S(2)	124.3(2)		
Cl(3)–Cu(3)–S(3)	127.4(2)		

$(NPr_4)_3[WS_4Cu_4Cl_5]$ (5a)

An ORTEP representation of the anionic structure is given in Fig. 4, and a set of selected bond distances and angles in Table 7. The overall arrangement of the anion results from the addition of four CuCl groups and a chlorine atom on the thiometallate, yielding a new cubane geometry with ***an additional face*** according to model I.

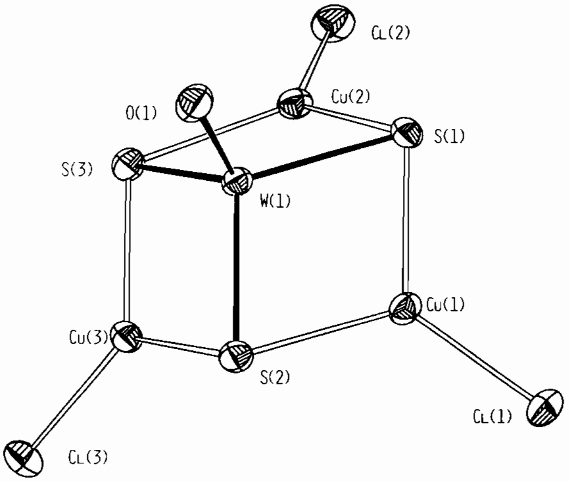

Fig. 3. ORTEP drawing (15% ellipsoids) of the lacunary cubane $[WOS_3Cu_3Cl_3]^{2-}$.

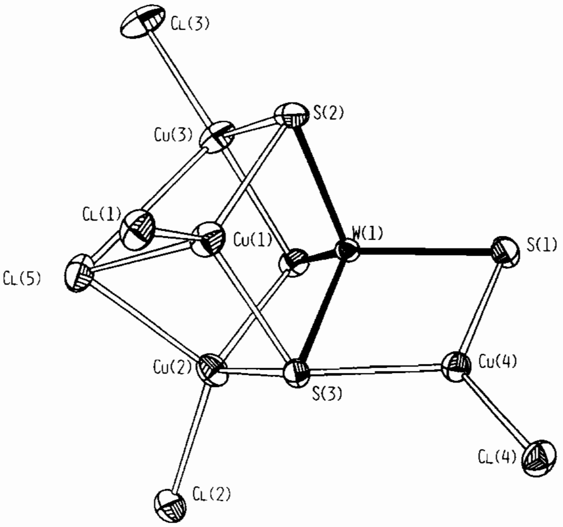

Fig. 4. ORTEP representation of $[WS_4Cu_4Cl_5]^{3-}$, a cubane with an additional face.

TABLE 7. Selected bond distances (Å) and angles (°) for the $[WS_4Cu_4Cl_5]^{3-}$ anion in **5a**

W(1)–S(1)	2.227(4)	W(1)–S(3)	2.242(5)
W(1)–S(2)	2.217(4)	W(1)–S(4)	2.246(5)
W(1)...Cu(1)	2.692(3)	W(1)...Cu(2)	2.693(2)
W(1)...Cu(3)	2.640(3)	W(1)...Cu(4)	2.643(2)
S(2)–W(1)–S(1)	110.7(2)	S(4)–W(1)–S(1)	109.7(2)
S(3)–W(1)–S(1)	108.6(2)	S(4)–W(1)–S(2)	109.0(2)
S(3)–W(1)–S(2)	109.6(2)	S(4)–W(1)–S(3)	109.2(2)
Cu(2)–W(1)–Cu(1)	74.13(9)	Cu(4)–W(1)–Cu(1)	95.29(8)
Cu(3)–W(1)–Cu(1)	75.79(9)	Cu(4)–W(1)–Cu(2)	100.14(7)
Cu(3)–W(1)–Cu(2)	76.23(9)	Cu(4)–W(1)–Cu(3)	170.96(8)
S(1)–Cu(4)	2.252(6)	S(3)–Cu(2)	2.348(5)
S(2)–Cu(1)	2.321(6)	S(3)–Cu(4)	2.268(5)
S(2)–Cu(3)	2.265(7)	S(4)–Cu(2)	2.300(5)
S(3)–Cu(1)	2.338(6)	S(4)–Cu(3)	2.281(6)
Cu(4)–S(1)–W(1)	72.3(1)		
Cu(1)–S(2)–W(1)	72.7(1)	Cu(2)–S(4)–W(1)	72.6(2)
Cu(3)–S(2)–W(1)	72.2(2)	Cu(3)–S(4)–W(1)	71.3(2)
Cu(3)–S(2)–Cu(1)	91.1(2)	Cu(3)–S(4)–Cu(2)	91.9(2)
Cu(1)–S(3)–W(1)	71.9(2)	Cu(4)–S(3)–W(1)	71.7(2)
Cu(2)–S(3)–W(1)	71.8(1)	Cu(4)–S(3)–Cu(1)	117.7(2)
Cu(2)–S(3)–Cu(1)	87.7(2)	Cu(4)–S(3)–Cu(2)	124.9(2)
Cu(1)–Cl(1)	2.184(6)	Cu(1)–Cl(5)	2.607(7)
Cu(2)–Cl(2)	2.211(5)	Cu(2)–Cl(5)	2.463(5)
Cu(3)–Cl(3)	2.157(6)	Cu(3)–Cl(5)	2.969(7)
Cu(4)–Cl(4)	2.142(5)		
S(3)–Cu(1)–S(2)	102.9(2)	Cl(5)–Cu(1)–S(2)	102.3(2)
Cl(1)–Cu(1)–S(2)	123.9(3)	Cl(5)–Cu(1)–S(3)	91.5(2)
Cl(1)–Cu(1)–S(3)	121.8(2)	Cl(5)–Cu(1)–Cl(1)	108.2(3)
S(4)–Cu(2)–S(3)	103.9(2)	Cl(5)–Cu(2)–S(3)	95.0(2)
Cl(2)–Cu(2)–S(3)	118.6(2)	Cl(5)–Cu(2)–S(4)	102.0(2)
Cl(2)–Cu(2)–S(4)	119.2(2)	Cl(5)–Cu(2)–Cl(2)	114.4(2)
S(4)–Cu(3)–S(2)	106.1(2)	Cl(5)–Cu(3)–S(2)	93.5(2)
Cl(3)–Cu(3)–S(2)	120.4(3)	Cl(5)–Cu(3)–S(4)	88.7(2)
Cl(3)–Cu(3)–S(4)	127.4(2)	Cl(5)–Cu(3)–Cl(3)	110.0(3)
Cl(4)–Cu(4)–S(1)	129.0(2)		
S(3)–Cu(4)–S(1)	106.8(2)		
Cl(4)–Cu(4)–S(3)	124.2(2)		
Cu(2)–Cl(5)–Cu(1)	79.5(2)		
Cu(3)–Cl(5)–Cu(1)	71.6(1)		
Cu(3)–Cl(5)–Cu(2)	73.9(2)		

The W atom has retained its initial tetrahedral geometry, with S–W–S angles in the range 108.6(2)–110.7(2)°. Sulfur atoms are present in the structure with three different coordinations. S(1) is bonded to the tungsten and to only one copper (Cu(4)), S(2) to the tungsten and to two coppers (Cu(1) and Cu(3)), S(4) to Cu(2) and Cu(3), and S(3) to the tungsten and three coppers (Cu(1), Cu(2), Cu(4)). In spite of the versatility of the bonding mode of the S atoms, the Cu–S–W angles remain in the short range, 71.3(2)–72.7(1)°, showing that the central WS_4 core can be considered as a rigid group. Conversely, the Cu–S–Cu angles are clearly dependent on the coordination of the Cu atoms. Two different geometries are observed for the four copper atoms.

(i) Cu(4) is distorted trigonal planar with Cu angles ranging from 106.8(2) to 129.0(2)°. The maximum deviation from the W(1)S(1)S(3)Cu(4)Cl(4) plane is 0.099 Å for the tungsten atom.

(ii) Cu(1), Cu(2) and Cu(3) are tetracoordinated. The mean Cu–S distance, 2.31[3] Å, is longer than the corresponding mean bond lengths of the trigonal Cu(4), 2.26[1] Å. This difference probably reflects a weakening of the Cu–S bond by increasing the coordination of the Cu atoms. Such an effect is also observed for the terminal Cu–Cl bonds, the Cu(4)–Cl(4) distance, 2.142(5) Å, being significantly shorter than Cu(3)–Cl(3) = 2.157(6), Cu(1)–Cl(1) = 2.184(6) and Cu(2)–Cl(2) = 2.211(5) Å.

The coordination of the three Cu atoms is achieved by the bridging Cl(5) atom through long Cu–Cl bonds ranging from 2.463(5) to 2.969(7) Å. This Cl(5) atom gives to the W(1)Cu(1)Cu(2)Cu(3)Cl(1)Cl(2)Cl(3)Cl(5) moiety a distorted cubic geometry. The main distortions arise from the W atom since its tetrahedral geometry constrains the S–W–S angles close to 109.5°, and also from the three edges bonded to the Cl(5) vertex which appear longer than the other edges of the cube. The rigidity of the WS_4 tetrahedron probably contributes most to the distortion of the cubane. Calculations of the six mean planes forming the six faces of the cube reveal that the maximum out of plane deviation is systematically obtained for an atom of the rigid group as shown in Table 8.

TABLE 8. Calculated mean-plane deviations in **5a**

Mean plane	Δ_{max} (Å)	Atom
W(1)S(2)S(3)Cu(1)	0.131	W(1)
W(1)S(2)S(4)Cu(3)	0.086	W(1)
W(1)S(3)S(4)Cu(2)	0.121	W(1)
S(2)Cu(1)Cu(3)Cl(5)	0.117	S(2)
S(3)Cu(1)Cu(2)Cl(5)	0.216	S(3)
S(4)Cu(2)Cu(3)Cl(5)	0.171	S(4)

Synthesis and reactivity

Formation of the cubane structure

Cubanes **4a** and **4b** were previously obtained by Müller *et al.* by reaction of $(NH_4)_2[MS_4]$ (M = Mo, W) with PPh_3 and $CuCl_2 \cdot 2H_2O$ [32]. In order to avoid the reduction step Cu(II) → Cu(I), compounds **1a**, **2a** and **2b** were prepared here by direct addition of CuCl to $[MS_4]^{2-}$ with excess of chloride.

$$[MS_4]^{2-} + 3CuCl + 3Cl^- \xrightarrow{CH_2Cl_2,\ \Delta} \underset{\textbf{1a, 2a, 2b}}{[MS_4Cu_3Cl_4]^{3-}} \quad (1)$$

In these preparations, the role of the cation associated with the additional chloride is important since with PPN^{+} *, NPr_4^{+} and NEt_4^{+} cubanes were still obtained, but not with the specific cation PPh_4^{+}. Instead of cubanes other compounds, $(PPh_4)_2[MS_4Cu_3Cl_3]$ [26, 27], having the same ratio Cu/M = 3, but the open structure (e), were isolated. These compounds were previously obtained by direct addition of CuCl on $(PPh_4)_2[MS_4]$ (M = Mo, W).

$$(PPh_4)_2[MS_4] + 3CuCl \longrightarrow (PPh_4)_2[MS_4Cu_3Cl_3] \qquad (2)$$

By comparison of eqns. (1) and (2), it can be postulated that $[MS_4Cu_3Cl_3]^{2-}$ could exist in solution as an intermediate species consisting of two isomeric forms in equilibrium, one close to the open structure (intermediate I), the other close to the cubane structure (intermediate II). The final product adopts the configuration most stabilized by the cation present in solution, cubane with NPr_4^{+} and NEt_4^{+}, open structure with PPh_4^{+}.

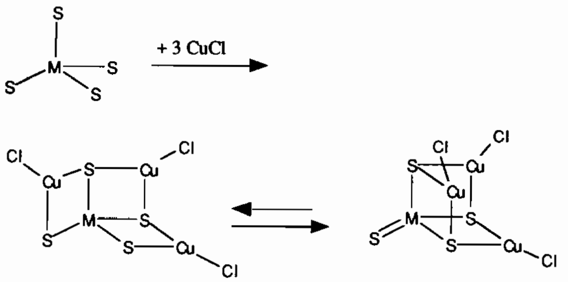

Intermediate I **Intermediate II**

In intermediate **II**, the relative positions of the Cu atoms allow the addition of a supplementary chlorine which can complete the tetrahedral geometry of copper atoms to yield the cubane structure

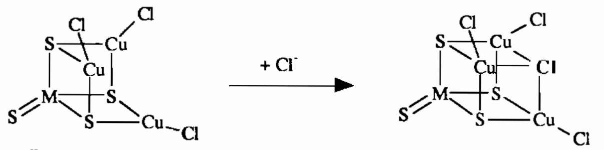

Intermediate III **2a, 2b**

Chloride ions added as NPr_4Cl have a specific role in the formation of the cubane structure. Compounds **3a** and **3b**, which were isolated *after* formation of the $[MS_4Cu_3Cl_4]^{3-}$ cubane, can be considered as cubanes with a missing chloro corner, since after elimination of cubane compounds **2a** and **2b**, the concentration of Cl^- ions in solution is poor leading to the formation of the chloro lacunary cubanes (f), **3a** and **3b**.

*$(PPN)_3[WS_4Cu_3Cl_4]$ was characterized from C and H analyses, UV–Vis and IR spectroscopic data.

Without addition of NPr_4Cl, reaction (1) led to compounds with the open structure (h), namely $(NPr_4)_2[MS_4Cu_4Cl_4]$ [39].

Reactivity of the cubane structure

In **2a** and **2b**, the three terminal chloro ligands were easily substituted by strong σ-donor ligands such as PPh_3 to give **4a** and **4b**. The three Cu atoms are strictly equivalent so, even with excess of **2a** or **2b**, attempts to isolate compounds resulting from partial substitution of Cl^- ligands failed.

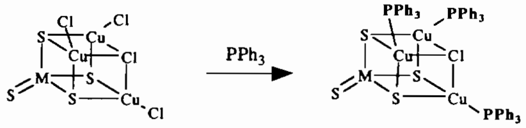

2a, 2b **4a, 4b**

In the type (g) cubane structure $[MS_4Cu_3Cl_4]^{3-}$, three edges of the central MS_4 tetrahedron are uncoordinated. Addition of a fourth CuCl group across one of these free edges led to **5a** and **5b** and to a compound of the same Cu/M = 4 ratio, $(NPr_4)_2[MS_4Cu_4Cl_4]$ [39]. Compounds **5a** and **5b** represent the first example of an extended cubane structure.

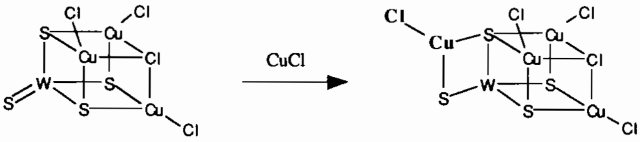

2a, 2b **5a,5b**

In a following paper we will report on a new lacunary dicubane $[MS_4Cu_5X_6]^{3-}$ (X = Cl, I) obtained by a similar route.

The cubane structure (g) has retained the reducing power of the parent thiometallate since addition of $(NPr_4)_2[CuCl_4]$ to **2a** and **2b** led to the diamagnetic **5a** and **5b** compounds (no EPR signal). The redox behaviour of the cubane structure probably arises from the presence of a double $W{=}S_t$ bond, reductant through the terminal sulfido, since Cu^{2+} ions are not reduced by $[WS_4Cu_3Cl_3]^{2-}$ which has the same Cu/M = 3 ratio but does not contain a $W{=}S_t$ terminal bond (open structure (e)).

Discussion of the structures

In this work, two new compounds having the cubane structure have been described. Regarding the crystallographic results, two structural features deserve discussion. Cubane structures **4a** and **4b** can be considered as deriving from the $[CuClPPh_3]_4$ cubane arrangement [47] by replacing a $CuCl_3PPh_3$ fragment by an MS_4 group. This substitution produces significant distortions in the structure.

In Table 9 are listed angles of the cubic fragment of various cubanes. Cubanes containing the WS_4 core

TABLE 9. Angles (°) in cubic fragments of various cubane structures

Compound	Cubic fragment	Angles	Mean
$[Cu_4Cl_4(PPh_3)_4]$· [47]	$[Cu_4Cl_4]$	79.71(6)–101.11(7)	89[6]
$[Cu_3(PPh_3)_3ClWS_4]$ [32]	$[WS_3ClCu_3]$	72.5(1)–108.2(1)	89[14]
$(NEt_4)_4[Cu_3Cl_4WS_4]Cl$ (**2b**)	$[WS_3ClCu_3]$	72.7(2)–109.4(2)	90[13]
$(NPr_4)_3[Cu_4Cl_5WS_4]$ (**5b**)	$[WS_3ClCu_3]$	71.3(2)–109.6(2)	89[14]

TABLE 10. W...Cu distances (Å) in various cubic fragments

Compound	W...Cu(tetrag.)	W...Cu(trig.)	Cu...Cu
$[Cu_4Cl_4(PPh_3)_4]$ [47]			3.31[14]
$[Cu_3(PPh_3)_3ClWS_4]$ [32]	2.72[2]		3.18[7]
$(NEt_4)_4[Cu_3Cl_4WS_4]Cl$ (**2b**)	2.80[2]		3.103[2]
$(NPr_4)_3[Cu_4Cl_5WS_4]$ (**5b**)	2.67[2]	2.643(2)	3.27[2]

are more distorted than the $[Cu_4Cl_4(PPh_3)_4]$ parent, probably because of the rigidity of the central WS_4 tetrahedron. The observed metal–metal distances vary considerably in the different clusters. These distances are presented in Table 10, averaged for metals in a similar environment. In $[Cu_4Cl_4(PPh_3)_4]$, the Cu···Cu separations are too long to allow any metal–metal interaction. The situation appears quite different when an MS_4 group replaces $CuCl_3PPh_3$. In the two compounds $[WS_4Cu_3L_3Cl]^{n-}$ ($L=PPh_3$, $n=0$; $L=Cl^-$, $n=3$), the W···Cu interaction increases with the σ donor power of the L ligand bonded to the Cu atom. This variation, together with the difficulty to prepare cubanes substituted by the CO π-acceptor ligand, agrees with the hypothesis of an electronic delocalization from Cu to W.

Acknowledgement

We are grateful to Dr R. Speel for helpful discussions.

References

1 R. H. Holm, *Chem. Soc. Rev., 10* (1981) 55.
2 D. Coucouvanis, *Acc. Chem. Rev., 14* (1981) 201.
3 A. Müller, E. Diemann, R. Jostes and H. Bögge, *Angew. Chem., Int. Ed. Engl., 20* (1981) 934.
4 A. Müller, W. Jaegermann and J. H. Enemark, *Coord. Chem. Rev., 46* (1982) 245.
5 B. A. Averill, *Struct. Bonding (Berlin), 53* (1983) 59.
6 M. Draganjac and T. B. Rauchfuss, *Angew. Chem., Int. Ed. Engl., 24* (1985) 742.
7 A. Müller, *Polyhedron, 5* (1986) 323.
8 D. Coucouvanis, A. Hadjikyriacou, M. Draganjac, M. G. Kanatzidis and O. Ileperuma, *Polyhedron, 5* (1986) 349.
9 A. Müller and E. Diemann, *Adv. Inorg. Chem. Radiochem., 31* (1987) 89.
10 M. R. DuBois, *Chem. Rev., 89* (1989) 1.
11 P. A. Eldredge and B. A. Averill, *J. Cluster Sci., 1* (1990) 269.
12 W. S. Ferguson, A. L. Lewis and S. J. Watson, *J. Agric. Sci., 33* (1943) 44.
13 N. F. Suttle, W. G. Hoekstra, J. W. Suttle, H. E. Ganther and W. Hertz, *Trace Element Metabolism in Animals*, University Park Press, Baltimore, MD, p. 612.
14 I. Bremner and C. F. Mills, *Philos. Trans. R. Soc. London, Ser. B, 294* (1981) 75.
15 A. Müller, M. Dartmann, C. Römer, W. Clegg and G. M. Sheldrick, *Angew. Chem., Int. Ed. Engl., 20* (1981) 1060; S. F. Gheller, P. A. Gazzana, A. F. Masters, R. T. C. Brownlee, M. J. O'Connor, A. G. Wedd, J. R. Rodgers and M. R. Snow, *Inorg. Chim. Acta, 54* (1981) 131.
16 S. R. Acott, C. D. Garner, J. R. Nicholson and W. Clegg, *J. Chem. Soc., Dalton Trans.,* (1983) 713.
17 A. Müller, E. Diemann, R. Jostes and H. Bögge, *Angew. Chem., Int. Ed. Engl., 20* (1981) 934.
18 A. Müller, U. Schimanski and J. Schimanski, *Inorg. Chim. Acta, 76* (1983) L245.
19 F. Sécheresse, M. Salis, C. Potvin and J. M. Manoli, *Inorg. Chim. Acta, 114* (1986) 19.
20 J. R. Nicholson, S. Boyde, C. D. Garner and W. Clegg, unpublished results.
21 C. Potvin, J. M. Manoli, F. Sécheresse and S. Marzak, *Inorg. Chem., 26* (1987) 4370.
22 C. Potvin, J. M. Manoli, F. Sécheresse and S. Marzak, *Inorg. Chim. Acta, 134* (1987) 9.
23 A. Müller, H. Bögge and U. Schimanski, *Inorg. Chim. Acta, 45* (1980) L249.
24 A. Müller, H. Bögge and E. Königer-Ahlborn, *Z. Naturforsch., Teil B, 34* (1979) 1698.
25 A. Müller, W. Jaegermann and W. Hellmann, *J. Mol. Struct., 100* (1983) 559.
26 W. Clegg, C. D. Garner and J. R. Nicholson, *Acta Crystallogr., Sect. C., 39* (1983) 552.
27 C. Potvin, J. M. Manoli, M. Salis and F. Sécheresse, *Inorg. Chim. Acta, 83* (1984) L19.
28 J. M. Manoli, C. Potvin, F. Sécheresse and S. Marzak, *Inorg. Chim. Acta, 150* (1988) 257.
29 Z. Huang, X. Lei, J. Liu, B. Kang, Q. Liu, M. Hong and H. Liu, *Inorg. Chim. Acta, 169* (1990) 25.
30 H. Liu, R. Cao, X. Lei, D. Wu, G. Wei, Z. Huang, M. Hong and B. Kang, *J. Chem. Soc., Dalton Trans.,* (1990) 1023.

31 W. Clegg, A. Beheshti and C. D. Garner, *Acta Crystallogr., Sect. C, 44* (1988) 170.
32 A. Müller, H. Bögge and U. Schimanski, *Inorg. Chim. Acta, 69* (1983) 5; *J. Chem. Soc., Chem. Commun.*, (1980) 91; A. Müller, H. Bögge, H. G. Tölle, R. Jostes, U. Schimanski and M. Dartmann, *Angew. Chem., Int. Ed. Engl., 19* (1980) 654.
33 A. Müller, H. Bögge and T. K. Hwang, *Inorg. Chim. Acta, 39* (1980) 71.
34 R. M. Doherty, C. R. Hubbard, A. D. Mighell, A. R. Siedle and J. M. Stewart, *Inorg. Chem., 18* (1979) 2991.
35 J. K. Stalick, A. R. Siedel, A. D. Mighell and C. R. Hubbard, *J. Am. Chem. Soc., 101* (1979) 2903.
36 W. Clegg, C. D. Scattergood and C. D. Garner, *Acta Crystallogr., Sect. C, 43* (1987) 786.
37 J. R. Nicholson, A. C. Flood, C. D. Garner and W. Clegg, *J. Chem. Soc., Chem. Commun.*, (1983) 1179.
38 J. M. Manoli, C. Potvin, F. Sécheresse and S. Marzak, *J. Chem. Soc., Chem. Commun.*, (1986) 1557.
39 F. Sécheresse, S. Bernès, F. Robert and Y. Jeannin, *J. Chem. Soc., Dalton Trans.*, (1991) 2875.
40 F. Sécheresse, F. Robert, S. Marzak, J. M. Manoli and C. Potvin, *Inorg. Chim. Acta, 182* (1991) 221.
41 F. Sécheresse, J. M. Manoli, C. Potvin and S. Marzak, *J. Chem. Soc., Dalton Trans.*, (1988) 3055.
42 A. Müller, E. Krickemeyer and H. Bögge, *Angew. Chem., Int. Ed. Engl., 25* (1986) 990.
43 S. Bernès, F. Sécheresse and Y. Jeannin, *Inorg. Chim. Acta, 191* (1992) 11.
44 N. Walker and D. Stuart, *Acta Crystallogr., Sect. A, 39* (1983) 158.
45 G. M. Sheldrick, *SHELXS 86*, a program for crystal structure determination, University of Göttingen, FRG, 1986.
46 D. J. Watkin, J. K. Carruthers and P. Betteridge, *CRYSTALS*, an advanced crystallographic program system, Chemical Crystallographic Laboratory, University of Oxford, UK, 1989.
47 M. R. Churchill and K. L. Kalra, *Inorg. Chem., 13* (1974) 1065.